Piezoelectricity above the Curie temperature? Combining flexoelectricity and functional grading to enable high-temperature electromechanical coupling

R. Mbarki,[1] N. Baccam,[2] Kaushik Dayal,[3] and P. Sharma[4]
[1]*Department of Mechanical Engineering, University of Houston, Houston, Texas 77204, USA*
[2]*Department of Mathematics, Southwestern University, Georgetown, Texas 78626, USA*
[3]*Department of Civil and Environmental Engineering, Carnegie Mellon University, Pittsburgh, Pennsylvania 15213, USA*
[4]*Department of Mechanical Engineering and Department of Physics, University of Houston, Houston, Texas 77204, USA*

(Received 1 December 2013; accepted 12 March 2014; published online 25 March 2014)

Most technologically relevant ferroelectrics typically lose piezoelectricity above the Curie temperature. This limits their use to relatively low temperatures. In this Letter, exploiting a combination of flexoelectricity and simple functional grading, we propose a strategy for high-temperature electromechanical coupling in a standard thin film configuration. We use continuum modeling to quantitatively demonstrate the possibility of achieving apparent piezoelectric materials with large and temperature-stable electromechanical coupling across a wide temperature range that extends significantly above the Curie temperature. With Barium and Strontium Titanate, as example materials, a significant electromechanical coupling that is potentially temperature-stable up to 900 °C is possible. © *2014 AIP Publishing LLC*. [http://dx.doi.org/10.1063/1.4869478]

A piezoelectric material couples electric fields with mechanical stress and deformation. It enables the conversion of stimuli and energy between electromagnetism and mechanics, and has important applications that range from energy harvesting to artificial muscles.[1] Perovskites such as Barium Titanate ($BaTiO_3$) and Lead Titanate ($PbTiO_3$) are two widely used materials that exhibit a fairly high electromechanical coupling.[2–4] The piezoelectricity in these materials, which are also ferroelectric, are driven by an asymmetric distribution of charges in the atomic unit cell. Above the Curie temperature (T_c), the crystal structure transforms to a centrosymmetric state, and both ferroelectricity and piezoelectricity disappear. For example, at $T_c = 120\,^{\circ}C$ in $BaTiO_3$, it transforms from a non-centrosymmetric tetragonal crystal to a centrosymmetric cubic crystal. The loss of piezoelectricity at such (relatively) low temperatures hinders their potential application to areas ranging from hypersonics to oil extraction, which require high-temperature energy harvesting, harsh environment sensing, and actuation, among others.

We exploit flexoelectricity as the first element of our strategy to go beyond this limitation. Flexoelectricity denotes the coupling between polarization and strain *gradients*; this is in contrast to piezoelectricity that relates polarization to strains. The difference between piezoelectricity and flexoelectricity can be readily observed from the following equation:

$$P_i = e_{ijk}S_{jk} + f_{ijkl}S_{jk,l}, \tag{1}$$

where, P_i is the electric polarization, S_{jk} is the strain tensor, e_{ijk} is the third order piezoelectric tensor, and f_{ijkl} is the fourth order flexoelectric tensor. Flexoelectricity is a property that is displayed by all dielectrics to some degree. Thus, in a centrosymmetric material, where the piezoelectric tensor $\boldsymbol{e}$ vanishes, non-uniform strains can still induce a polarization. Flexoelectricity is mediated through the fourth-order tensor $\boldsymbol{f}$, and unlike $\boldsymbol{e}$, symmetry principles permit its existence in all types of crystal structure and not just non-centrosymmetric crystals. For instance, while $BaTiO_3$ will cease to be piezoelectric above $T_c = 120\,^{\circ}C$, it can still display flexoelectricity.

Flexoelectricity has recently received much attention, e.g., it suggests tantalizing possibilities such as creating effectively piezoelectric materials without using piezoelectrics.[5–10] In a recent work, Chandratre and Sharma showed, using quantum calculations, that merely by creating triangular holes in graphene nano ribbons, flexoelectricity enabled the ensuing structure to behave like a piezoelectric.[11] Their central idea is simple and the present work takes advantage of the following observation. Consider a material consisting of two different non-piezoelectric dielectric materials. Even under uniform stress, the difference in the material properties at the interfaces causes strain gradients. Those gradients will induce polarization due to the flexoelectric effect. In a nanostructure, it is possible to induce sufficiently large strain gradients that flexoelectricity-induced polarization is significant. Thus, such a nanostructure will exhibit an overall electromechanical coupling under uniform stress behaving like a piezoelectric material. Accordingly, predicated on this same concept, a functionally graded non-piezoelectric material should appear to behave like a piezoelectric. A key requirement, however, is that the geometry should be non-centrosymmetric. For example, uniformly stressed composites with spherical inclusions will exhibit spatially varying polarization due to flexoelectricity, however, the average polarization will vanish. Similarly, bilayer superlattices will not exhibit an apparent piezoelectric response while a trilayer superlattice will. Following this reasoning, compositionally graded thin films must have asymmetric grading.

Several other works have studied flexoelectricity and its implications:, e.g., Ref. 12 studied the impact of flexoelectricity on the dielectric properties and T_c of ferroelectrics,[7,8] fabricated flexoelectric composites, and[9,10] investigated the renormalization in properties of ferroelectric nanostructures due to the flexoelectric effect and analyzed consequent

 © 2014 AIP Publishing LLC

This article is copyrighted as indicated in the article. Reuse of AIP content is subject to the terms at: http://scitation.aip.org/termsconditions. Downloaded to IP: 128.2.73.68 On: Wed, 26 Mar 2014 17:24:27

size effects. Composition grading has also been studied in relation to polarization coupling in ferroelectrics—e.g., Refs. 13 and 14. The work in Ref. 15 showed that flexoelectricity plays an important role in increasing the pyroelectric property of graded ferroelectric materials and[16] investigated the large built-in electric fields in graded ferroelectric thin films due to flexoelectric coupling. In our previous work,[5] we have computationally demonstrated the possibility of designing such composites through suitable topologies, material property differences, and the selection of optimum feature sizes. Such topologies can be challenging to realize, however, non-piezoelectric tapered pyramidal structures on substrate that effectively act as piezoelectric materials have been fabricated in experimental studies in Refs. 7, 17, and 18. Recent reviews of flexoelectricity include.[19–21]

This leads us to the second element of our strategy, namely, functional grading. We emphasize that $\boldsymbol{f}$ is temperature-dependent. In particular, it roughly follows the dielectric constant of the material, which is itself a measure of the mobility of charges in the atomic unit cell. Therefore, $\boldsymbol{f}$ is larger in high-dielectric materials—such as ferroelectric perovskites—and also gets much larger near T_c. However, T_c can be tuned by changing the composition of the material, e.g., Ref. 22 experimentally tuned the composition of $Ba_{0.67}Sr_{0.33}TiO_3$ to bring T_c to room temperature. Compositional grading in a ferroelectric film provides a heterogeneous body with T_c a function of spatial position. Hence, for a broad range of ambient temperatures, there will be some portion of the film whose local value of T_c coincides with the ambient temperature. That portion of the film will have a high flexoelectric coefficient. Together with the notion that a heterogeneous flexoelectric medium behaves like an apparent piezoelectric and that both flexoelectric and dielectric properties are likely to peak in at least one layer of the graded thin film structure, a high apparent piezoelectric response may be expected across a wide range of temperature. That enables two positive features: first, a higher effective flexoelectric response over a broad range of temperatures, and second, temperature stability of the flexoelectric response. Key elements of this strategy follow.[23] Additionally, even when the entire film is above the local T_c, the use of heterogeneous films provides a simple route to applying an inhomogeneous strain that is required for flexoelectricity. Figure 1 presents a schematic description of the dielectric permittivity variation within each layer.

The schematic of the thin film is shown in Figure 2. We consider a candidate grading geometry as shown in the figure. The grading goes from pure Barium Titanate to pure Strontium Titanate.

We model the thin film using a continuum approach. Denote the volume occupied by the film as V, and it is subject to an applied traction $\boldsymbol{\sigma}^0$ on the boundary ∂V. The free energy of the system is then given by the following expression:

$$F = \underbrace{\int_V w(\boldsymbol{P}, \nabla \boldsymbol{u}, \nabla \boldsymbol{P}, \nabla\nabla \boldsymbol{u})\, dV}_{\text{internal energy}} + \underbrace{\frac{\epsilon_0}{2}\int_{\mathbb{R}^3} |\nabla \Phi|^2\, dV}_{\text{electrostatic energy}} - \underbrace{\int_{\partial V} \boldsymbol{\sigma}^0 \cdot \boldsymbol{u}\, dS}_{\text{boundary work}}. \quad (2)$$

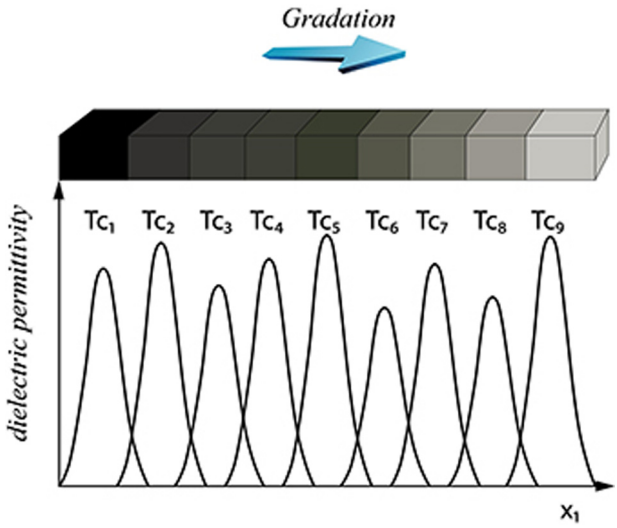

FIG. 1. Schematic variation of dielectric permittivity with temperature. When the ambient temperature is T_{c_1}, the dielectric permittivity has a spatial variation given by the curve with the label T_{c_1}, and similarly when the ambient temperatures are $T_{c_2}, T_{c_3}, \ldots$.

The notation above is as follows: $\boldsymbol{P}$ is the polarization vector field, $\boldsymbol{u}$ is the displacement vector field, and Φ is the electric potential field. Therefore, $\nabla \boldsymbol{u}$, $\nabla\nabla \boldsymbol{u}$, and $\nabla \boldsymbol{P}$ are, respectively, the strain, strain gradient, and polarization gradient fields.

The electric potential is obtained from the solution of the electrostatic equation

$$-\epsilon_0 \Phi_{,ii} + P_{i,i} = 0 \text{ in } V, \quad (-\epsilon_0 \Phi_{,i} + P_i) n_i = 0 \text{ on } \partial V. \quad (3)$$

We use index notation with implied summations here and below. We assume that there are no free charges. Under these electrical boundary conditions, the field is confined to the film and there are no stray fields external to the film. Therefore, we can simplify the electrostatic energy to read $\frac{\epsilon_0}{2}\int_V |\nabla \Phi|^2\, dV$.

In this Letter, we are not concerned with ferroelectric switching and related phenomena. The key feature of ferroelectrics that is relevant to the current calculation is the behavior of the dielectric permittivity, e.g., that it is

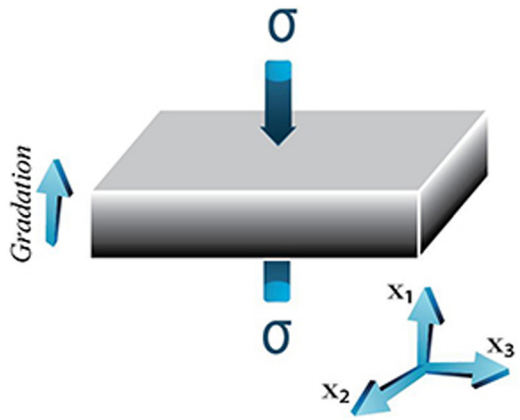

FIG. 2. Functionally graded thin film constructed from Barium Titanate and Strontium Titanate with grading through the thickness.

This article is copyrighted as indicated in the article. Reuse of AIP content is subject to the terms at: http://scitation.aip.org/termsconditions. Downloaded to IP: 128.2.73.68 On: Wed, 26 Mar 2014 17:24:27

unbounded at T_c, has the correct temperature variation, and so on. While electrostriction can have an important effect on T_c itself, we have found numerically that, beyond T_c, the *electromechanical coupling* is relatively unaffected and accordingly left out of our calculations. We linearize about the equilibrium state, and think now of $\boldsymbol{P}$ as the polarization relative to the spontaneous polarization in the material. The energy density w is then written[24,25]

$$w = \frac{1}{2}a_{ij}(x,T)P_iP_j + \frac{1}{2}b_{ijkl}P_{i,j}P_{k,l} + \frac{1}{2}c_{ijkl}(x)u_{i,j}u_{k,l} + d_{ijkl}P_{i,j}u_{k,l} + f_{ijkl}(x)u_{j,kl}P_i + \frac{1}{2}g_{ijklmn}u_{i,jk}u_{l,mn}. \quad (4)$$

Since the film is graded, we assume that the tensors $\boldsymbol{c}$ and $\boldsymbol{f}$ are position-dependent. Further, $\boldsymbol{a}$ is both position- and temperature-dependent, and we assume the variation $a_{ij}(x,T) = a_0(T - T_c(x))\delta_{ij}$ following.[23]

The governing equations can now be obtained by minimizing the free energy while subject to the electrostatic constraint

$$\begin{aligned} a_{ij}(x,T)P_j - h_{ijkl}(x)u_{j,kl} - b_{ijkl}P_{k,lj} + \Phi_i &= 0 \\ \left(c_{ijkl}(x)u_{k,l} + \left(h_{ijkl}(x)P_l\right)_k - g_{ijklmn}u_{l,mnk}\right)_j &= 0 \\ -\epsilon_0\Phi_{,ii} + P_{i,i} &= 0, \end{aligned} \quad (5)$$

subject to boundary conditions on ∂V

$$\begin{aligned} \left(b_{ijkl}P_{k,l} + h_{ijkl}(x)u_{k,l}\right)n_j &= 0 \\ \left(c_{ijkl}(x)u_{k,l} + \left(h_{ijkl}(x)P_l\right)_k - g_{ijklmn}u_{l,mnk}\right)n_j &= \sigma_i^o \\ \left(f_{ijkl}(x)P_l + g_{ijklmn}u_{l,mn}\right)n_jn_k &= 0 \\ \left(-\epsilon_0\Phi_{,i} + P_i\right)n_i &= 0. \end{aligned} \quad (6)$$

Here, $h_{ijkl} = d_{ijkl} - f_{ijkl}$.

The tetragonal symmetry of the barium titanate enables us to assume various components of the material property tensors to be 0. From this, and the fact that quantities vary only along the x_1 direction, we can assume that $\boldsymbol{P} = (P_1, 0, 0)$, and the only non-zero strains components are $u_{2,2} = u_{3,3}$ and $u_{1,1}$. For clarity, we use the following notation: $a_{11} = a$, $b_{1111} = b$, $h_{1111} = h_1$, $h_{1122} = h_2$, $c_{1111} = c_1$, $c_{1122} = c_2$, $g_{111111} = g_1$, $g_{111221} = g_2$, and $f_{1111} = f$.

The values of various material properties for pure Barium Titanate and Strontium Titanate are listed in Table I. We assume the rule of mixtures to compute the values of material properties for compositions between these extremes. The constants g_1 and g_2 are given in Ref. 25 and are assumed to be uniform.

TABLE I. Material properties.

	$BaTiO_3$	$SrTiO_3$
a_{11} (Nm^2/C^2)[23]	$6.6 \times 10^5(T - 110)$	$1.41 \times 10^6(T + 253)$
c_{1111} (N/m^2)[26,27]	275×10^9	350×10^9
c_{1122} (N/m^2)[26,27]	179×10^9	100×10^9
b_{1111} (Nm^4/C^2)	10^{-7}	10^{-7}
f_{1111} (C/m)[28,29]	0.35×10^{-9}	0.2×10^{-9}
f_{1122} (C/m)[18]	5×10^{-6}	7×10^{-9}

The film has thickness $H = 20$ nm and the equations are to be solved over $|x_1| < \frac{H}{2}$. The symmetry-motivated reductions lead to the simplified governing equations for the interior of the film

$$\begin{aligned} aP_1 - bP_{1,11} - h_1u_{1,11} - 2h_2u_{2,21} + \Phi_{,1} &= 0 \\ \left(c_1u_{1,1} + 2c_2u_{2,2} + (h_1P_1)_{,1} - g_1u_{1,111} - 2g_2u_{2,211}\right)_{,1} &= 0 \\ c_2u_{1,1} + (c_1 + c_2)u_{2,2} + (h_2P_1)_{,1} - g_2u_{1,111} - 2g_2u_{2,211} &= 0 \\ -\epsilon_0\Phi_{,11} + P_{1,1} &= 0. \end{aligned} \quad (7)$$

The boundary conditions at $x_1 = \pm\frac{H}{2}$ are

$$\begin{aligned} bP_{1,1} + h_1u_{1,1} + 2h_2u_{2,2} &= 0 \\ c_1u_{1,1} + 2c_2u_{2,2} + (h_1P_1)_{,1} - g_1u_{1,111} - 2g_2u_{2,211} &= \sigma^0 \\ fP_1 + g_1u_{1,11} + 2g_2u_{2,21} &= 0 \\ -\epsilon_0\Phi_{,1} + P_1 &= 0. \end{aligned} \quad (8)$$

To obtain the effective piezoelectric behavior of the film, we impose the uniform traction σ^0 on the boundary and numerically solve the governing equations to find the net polarization. Given the linearity of the equations, we define the ratio between these quantities as the effective piezoelectric coefficient d_{33}.

Figure 3 presents the key findings of this letter. The blue solid line is the piezoelectric coefficient of (ungraded) bulk Barium Titanate normalized with respect to the value at room temperature. Below T_c, the piezoelectric coefficient of the (ungraded) bulk Barium Titanate varies with temperature. Above T_c, as expected, this piezoelectric coefficient becomes zero and the electromechanical coupling vanishes. The red curve is the apparent piezoelectric coefficient obtained from the functionally graded thin film. It is also normalized with respect to the bulk value of Barium Titanate at room temperature. The functionally graded thin film produces an electric polarization equivalent to about 25% of conventional Barium Titanate for through-thickness grading. Notably, however, the apparent piezoelectricity is retained well beyond T_c and is stable across a broad range. The piezoelectric coefficient of Quartz, a "standard" piezoelectric material, is also marked. With through-thickness grading, our

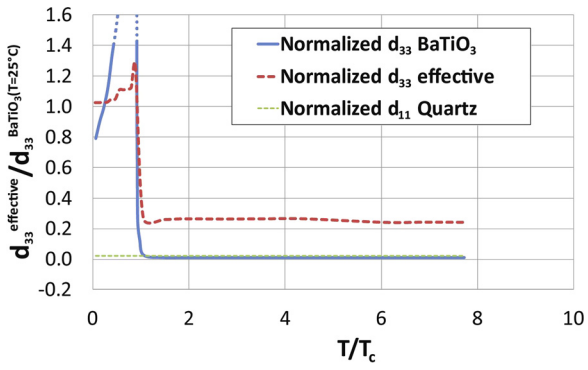

FIG. 3. Variation of normalized piezoelectric coefficient of Barium Strontium Titanate graded thin film as a function of the normalized temperature. The grading is in the thickness direction. Temperature normalization is with respect to unstrained $BaTiO_3$: 120 °C.

This article is copyrighted as indicated in the article. Reuse of AIP content is subject to the terms at: http://scitation.aip.org/termsconditions. Downloaded to IP: 128.2.73.68 On: Wed, 26 Mar 2014 17:24:27

strategy yields an apparent piezoelectric response that is almost three times larger.

The compositional grading geometry proposed here is readily achievable with available growth techniques for ferroelectric thin films.

Kaushik Dayal acknowledges support from ARO Numerical Analysis (YI W911NF-12-1-0156), AFOSR Computational Mathematics (YI FA9550-12-1-0350), and NSF Mechanics of Materials (CAREER 1150002). Pradeep Sharma gratefully acknowledges support from NSF CMMI 0969086 and IMI center IIMEC 0844082.

[1]J. Yang, Appl. Mech. Rev. **59**(6), 335 (2006).
[2]A. Schaefer, H. Schmitt, and A. Dorr, Ferroelectrics **69**, 253 (1986).
[3]M. Davis, D. Damjanovic, and N. Setter, J. Appl. Phys. **100**, 084103 (2006).
[4]D. Berlincourt and H. Jaffe, Phys. Rev. **111**, 143–148 (1958).
[5]N. D. Sharma, R. Maranganti, and P. Sharma, J. Mech. Phys. Solids **55**, 2328 (2007).
[6]N. D. Sharma, C. M. Landis, and P. Sharma, J. Appl. Phys. **108**, 024304 (2010).
[7]J. Y. Fu, W. Zhu, N. Li, and L. E. Cross, J. Appl. Phys. **100**, 024112 (2006).
[8]J. Fousek, L. E. Cross, and D. B. Litvin, Mater. Lett. **39**, 287–291 (1999).
[9]E. A. Eliseev, A. N. Morozovska, M. D. Glinchuk, and R. Blinc, Phys. Rev. B **79**, 165433 (2009).
[10]E. A. Eliseev and A. N. Morozovska, J. Mater. Sci. **44**, 5149 (2009).
[11]S. Chandratre and P. Sharma, Appl. Phys. Lett. **100**, 023114 (2012).
[12]G. Catalan, L. J. Sinnamon, and J. M. Gregg, J. Phys. Condens. Matter **16**, 2253 (2004).
[13]M. B. Okatan, J. V. Mantese, and S. P. Alpay, Phys. Rev. B **79**, 174113 (2009).
[14]J. V. Mantese, N. W. Schubring, A. L. Micheli, M. P. Thompson, R. Naik, G. W. Auner, I. B. Misirlioglu, and S. P. Alpay, Appl. Phys. Lett. **81**(6), 1068 (2002).
[15]M. Marvan, P. Chvosta, and J. Fousek, Appl. Phys. Lett. **86**(22), 221922 (2005).
[16]J. Karthik, R. V. K. Mangalam, J. C. Agar, and L. W. Martin, Phys. Rev. B **87**, 024111 (2013).
[17]L. E. Cross, J. Mater. Sci. **41**, 53 (2006).
[18]W. Ma and L. E. Cross, Appl. Phys. Lett. **88**, 232902 (2006).
[19]A. K. Tagantsev, V. Meunier, and P. Sharma, MRS Bull. **34**, 643 (2009).
[20]P. V. Yudin and A. K. Tagantsev, Nanotechnology **24**, 432001 (2013).
[21]P. Zubko, G. Catalan, and A. K. Tagantsev, Annu. Rev. Mater. Res. **43**, 387–421 (2013).
[22]W. Ma and L. E. Cross, Appl. Phys. Lett. **81**, 3440 (2002).
[23]M. El-Naggar, K. Dayal, D. G. Goodwin, and K. Bhattacharya, J. Appl. Phys. **100**, 114115 (2006).
[24]R. D. Mindlin, Int. J. Solids Struct. **8**, 369 (1972).
[25]R. Maranganti, N. D. Sharma, and P. Sharma, Phys. Rev. B **74**, 014110 (2006).
[26]J. D. Freire and R. S. Katiyar, Phys. Rev. B **37**, 2074 (1988).
[27]E. Poindexter and A. A. Glardini, Phys. Rev. **110**, 1069 (1958).
[28]J. Hong, G. Catalan, J. F. Scott, and E. Artacho, J. Phys. Condens. Matter **22**, 112201 (2010).
[29]P. Zubko, G. Catalan, A. Buckley, P. R. L. Welche, and J. F. Scott, Phys. Rev. Lett. **99**, 167601 (2007).

This article is copyrighted as indicated in the article. Reuse of AIP content is subject to the terms at: http://scitation.aip.org/termsconditions. Downloaded to IP: 128.2.73.68 On: Wed, 26 Mar 2014 17:24:27